

## Supporting Information

### **G-Quadruplex-Guided Cisplatin Triggers Multiple Pathways in Targeted Chemotherapy and Immunotherapy**

Tian-Zhu Ma,<sup>a</sup> Liu-Yi Liu,<sup>a</sup> You-Liang Zeng,<sup>a</sup> Ke Ding,<sup>c</sup> Hang Zhang,<sup>a</sup> Wenting Liu,<sup>\*a</sup> Qian Cao,<sup>a</sup> Wei Xia,<sup>a</sup> Xushen Xiong,<sup>\*c</sup> Chao Wu,<sup>\*b</sup> Zong-Wan Mao<sup>\*a</sup>

<sup>a</sup> MOE Key Laboratory of Bioinorganic and Synthetic Chemistry, School of Chemistry, IGCME, GBRCE for Functional Molecular Engineering, Sun Yat-Sen University, Guangzhou 510275, P. R. China

<sup>b</sup> Department of Neurology, The First Affiliated Hospital, Guangdong Provincial Key Laboratory of Diagnosis and Treatment of Major Neurological Diseases, National Key Clinical Department and Key Discipline of Neurology, Sun Yat-sen University, Guangzhou 510080, P. R. China

<sup>c</sup> The Second Affiliated Hospital & Liangzhu Laboratory, Zhejiang University School of Medicine, Hangzhou 311121, P. R. China. E-mail: xiongxs@zju.edu.cn

\*Corresponding Author(s): liuwenting@mail.sysu.edu.cn; xiongxs@zju.edu.cn;  
wuch35@mail.sysu.edu.cn; cesmzw@mail.sysu.edu.cn

# Contents

## Experimental Procedures

**Scheme S1.** The synthesis pathways of **CP**, **TP** and **DP**.

**Fig. S1**  $^1\text{H}$  NMR spectrum of **CP** in  $\text{DMSO-}d_6$ .

**Fig. S2**  $^{13}\text{C}$  NMR spectrum of **CP** in  $\text{DMSO-}d_6$ .

**Fig. S3** Mass spectrum of **CP**.

**Fig. S4**  $^1\text{H}$  NMR spectrum of **TP** in  $\text{DMSO-}d_6$ .

**Fig. S5**  $^{13}\text{C}$  NMR spectrum of **TP** in  $\text{DMSO-}d_6$ .

**Fig. S6** Mass spectrum of **TP**.

**Fig. S7**  $^1\text{H}$  NMR spectrum of **DP** in  $\text{DMSO-}d_6$ .

**Fig. S8**  $^{13}\text{C}$  NMR spectrum of **DP** in  $\text{DMSO-}d_6$ .

**Fig. S9** Representative structure of the 1:1 **CP**-c-MYC, VEGF and MYT1L complex.

**Fig. S10** (a) Thermal stabilization of MYT1L with **CP**, **TP**, **DP** and **PyPDS** while competing with increasing ratios of ds-12CT for binding to ligands.

**Fig. S11** ESI-MS of c-MYC, VEGF, MYT1L and dsDNA interacting with **CP**, **TP** and **DP**.

**Fig. S12** The amount of Pt in cell, nucleus and the amount of Pt in the genomic DNA of MDA-MB-231 cells after treated with different concentrations of **CP**, **TP** and **DP** for 24 h.

**Fig. S13** Distribution on chromosomes and GO enrichment of target gene.

**Fig. S14** (a) Venn diagram of the effects of compounds on genes. (b) Pie chart of the proportion of G4 deletions in whole-genome sequencing in the **CP** group.

**Fig. S15** Heatmap diagram of Pearson correlation coefficients between the RNA-seq samples.

**Fig. S16** Cluster analysis and Heatmap displayed the overview of the differentially expressed genes (DEGs) induced by **CP**, **TP**, **DP** and **PyPDS** for 24 h.

**Fig. S17** Volcano plots showing the DEGs in MDA-MB-231 cells treated with **CP** for 24 h.

**Fig. S18** Volcano plots showing the DEGs in MDA-MB-231 cells treated with **TP** for 24 h.

**Fig. S19** Volcano plots showing the DEGs in MDA-MB-231 cells treated with **DP** for 24 h.

**Fig. S20** Volcano plots showing the DEGs in MDA-MB-231 cells treated with **PyPDS** for 24 h.

**Fig. S21** GO enrichment analysis of DEGs.

**Fig. S22** KEGG enrichment analysis of differentially expressed genes after **CP**, **TP**, **DP** and **PyPDS**

treated for 24 h.

**Fig. S23** GSEA reveals positive enrichment of genes altered in cells subjected after **CP**, **TP**, **DP** and **PyPDS** treated.

**Fig. S24** The impact of different inhibitors on cell death induced by compounds.

**Fig. S25** Un-cropped western blotting images of Fig. 2f.

**Fig. S26** Un-cropped western blotting images of Fig. 3g.

**Fig. S27** Un-cropped western blotting images of Fig. 4g.

**Fig. S28** (a) Representative photographs of mice in the **CP** group at 24 days before sacrifice. (b) Volume changes of primary and distant tumors (n=4). Errors are s.d. (n≥3). (c-e) the secretion of cytokines (cGAMP, IL-18 and IL-1β) in serum on Day 16.

**Fig. S29** Hematoxylin and eosin (H&E) staining of the main organs from mice with different treatment.

**Table S1-3** The representative docked free energies of the docking models between **CP** and c-MYC, VEGF, MYT1L G4 DNA.

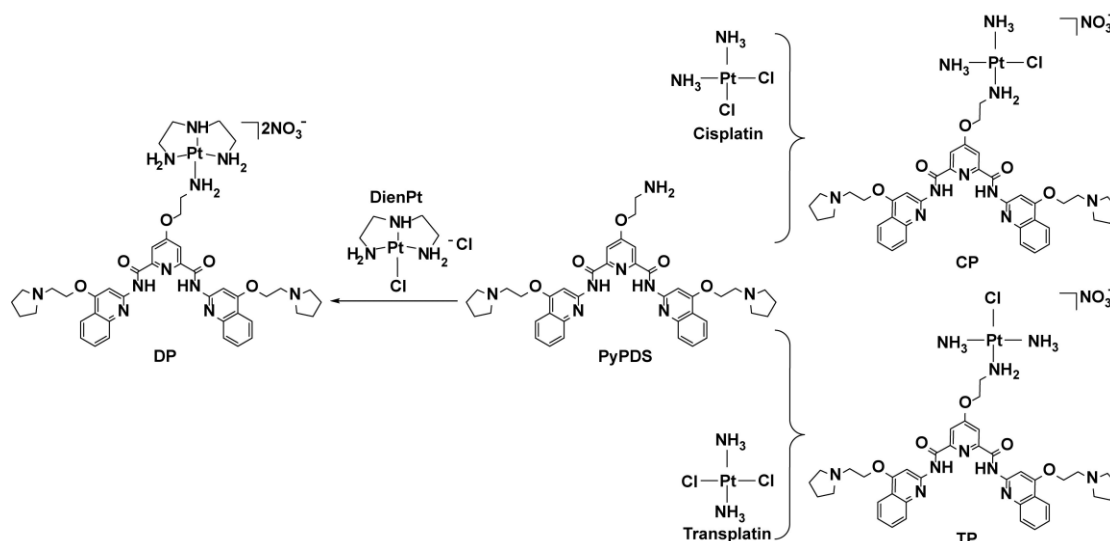
**Table S4** List of DNA sequences used in this research.

**Table S5.** The nearest gene of ChromHMM annotation.

**Table S6.** The Quadruplex forming G-Rich Sequences (QGRS) in the significant enrichment genes in the **CP** group.

**Table S7.** The **CP** group had the highest proportion of G4 deletions in whole-genome sequencing.

**Table S8.** The Quadruplex forming G-Rich Sequences (QGRS) in the genes of which the expression was significantly regulated by **CP** in the RNA-seq studies.



**Scheme S1.** The synthesis pathways of **CP**, **TP** and **DP**.

**Synthesis and Characterization.** As shown in Scheme S1, **PyPDS** was synthesized with reference to a previous study<sup>1</sup>.

The synthesis of cis- [Pt (NH<sub>3</sub>)<sub>2</sub>(PyPDS)Cl]NO<sub>3</sub> (**CP**), cisplatin (30.0 mg, 0.1 mmol, 1.0 eq.) and AgNO<sub>3</sub> (17 mg, 0.1 mmol, 1.0 eq.) were prepared in DMF (6 mL) under nitrogen protection at 35 °C in the dark and stirred for 12 h. After the reaction, the supernatant was filtered, **PyPDS** (70.0 mg, 0.1 mmol, 1.0 eq.) was added, and stirring was continued under nitrogen protection at 60 °C for 48 h in the dark. After cooling to room temperature, the samples were dried under vacuum and purified by HPLC to give the product (10.0 mg, yield 10%). ESI-MS (m/z): [**CP**+3H]<sup>3+</sup> calcd. for C<sub>39</sub>H<sub>52</sub>N<sub>10</sub>O<sub>5</sub>PtCl, 323.77; found: 323.78. [**CP**+2H]<sup>2+</sup> calcd. for C<sub>39</sub>H<sub>51</sub>N<sub>10</sub>O<sub>5</sub>PtCl, 485.16; found: 485.17. [**CP**+H]<sup>+</sup> calcd. for C<sub>39</sub>H<sub>50</sub>N<sub>10</sub>O<sub>5</sub>PtCl, 969.32; found: 969.33. <sup>1</sup>H NMR (400 MHz, DMSO-*d*<sub>6</sub>) δ 12.07 (s, 2H), 8.18 (d, *J* = 8.0 Hz, 2H), 8.17 (s, 2H), 8.12 (s, 2H), 7.97 (d, *J* = 4.0 Hz, 2H), 7.95 (d, *J* = 4.0 Hz, 2H), 7.79 (t, *J* = 8.0 Hz, 2H), 7.56 (t, *J* = 8.0 Hz, 2H), 4.51 – 4.56 (m, 3H), 4.50 (s, 2H), 4.47 (m, 4H), 4.41 (b, 3H), 3.99 (s, 2H), 3.21 (s, 4H), 2.83 (s, 8H), 1.79 (s, 8H). <sup>13</sup>C NMR (100 MHz, DMSO-*d*<sub>6</sub>) δ 167.25, 163.72, 162.46, 152.85, 151.56, 147.52, 131.15, 127.39, 125.25, 122.32, 119.66, 112.72, 95.52, 67.77, 63.55, 54.65, 54.07, 23.60.

Synthesis of trans- [Pt (NH<sub>3</sub>)<sub>2</sub>(PyPDS)Cl]NO<sub>3</sub> (**TP**): The synthesis method was the same as that for **CP**, except that the reactant replaced cisplatin with transplatin. [**TP**+3H]<sup>3+</sup> calcd. for C<sub>39</sub>H<sub>52</sub>N<sub>10</sub>O<sub>5</sub>PtCl, 323.77; found: 323.78. [**TP**+2H]<sup>2+</sup> calcd. for C<sub>39</sub>H<sub>51</sub>N<sub>10</sub>O<sub>5</sub>PtCl, 485.16; found:

485.17.  $[\text{TP}+\text{H}]^+$  calcd. for  $\text{C}_{39}\text{H}_{50}\text{N}_{10}\text{O}_5\text{PtCl}$ , 969.32; found: 969.33.  $^1\text{H}$  NMR (400 MHz,  $\text{DMSO}-d_6$ )  $\delta$  12.09 (s, 2H), 8.35 (s, 2H), 8.14 (s, 2H), 8.12 (s, 2H), 7.99 (s, 2H), 7.95 (d,  $J = 4.0$  Hz, 2H), 7.79 (t,  $J = 8.0$  Hz, 2H), 7.55 (t,  $J = 8.0$  Hz, 2H), 4.55 (s, 2H), 4.43 (t,  $J = 4.0$  Hz, 4H), 4.10 (s, 6H), 3.84 (b, 2H), 3.04 (t,  $J = 4.0$  Hz, 4H), 2.65 (s, 8H), 1.73 (s, 8H).  $^{13}\text{C}$  NMR (100 MHz,  $\text{DMSO}-d_6$ )  $\delta$  165.41, 163.73, 162.56, 152.91, 151.55, 147.52, 131.09, 127.40, 125.20, 122.22, 119.69, 112.76, 95.47, 68.49, 63.54, 54.68, 54.26, 23.72.

The synthesis of  $[\text{Pt}(\text{dien})(\text{PyPDS})](\text{NO}_3)_2$  (**DP**): DienPt-Cl (Dien = diethylenetriamine) was synthesized as described previously<sup>2</sup>. DienPt-Cl (37.0 mg, 0.1 mmol, 1.0 eq.) and  $\text{AgNO}_3$  (34.0 mg, 0.2 mmol, 2.0 eq.) were dissolved in 5 ml DMF. After the reaction was protected by nitrogen at room temperature for 12 h in the dark, the residue was filtered, and 5 ml of **PyPDS** (70.0 mg, 0.1 mmol, 70 mg) solution was dropped into it. The reaction was protected by nitrogen at 50 °C for 48 h in the dark, the reaction solution was filtered, the solid was washed three times with methanol, and the methanol solution was collected and dried. The product was freeze dried to obtain a pure product (10.0 mg, yield 10%).  $^1\text{H}$  NMR (400 MHz,  $\text{DMSO}-d_6$ )  $\delta$  12.09 (s, 2H), 8.18 (t,  $J = 8.0$  Hz, 2H), 8.13 (d,  $J = 4.0$  Hz, 2H), 8.09 (b, 2H), 8.00 (s, 2H), 7.95 (t,  $J = 8.0$  Hz, 2H), 7.80 (t,  $J = 8.0$  Hz, 2H), 7.56 (t,  $J = 8.0$  Hz, 2H), 5.68 (b, 2H), 5.51 (b, 2H), 4.51 (m, 6H), 3.59 (b, 2H), 3.10 (d,  $J = 4.0$  Hz, 2H), 2.91 (s, 8H), 2.68 (m, 8H), 1.81 (s, 8H).  $^{13}\text{C}$  NMR (100 MHz,  $\text{DMSO}-d_6$ )  $\delta$  170.44, 164.62, 161.71, 152.84, 150.53, 148.07, 131.17, 127.38, 125.27, 122.38, 119.63, 112.50, 95.52, 54.59, 53.45, 50.83, 45.62, 19.98.



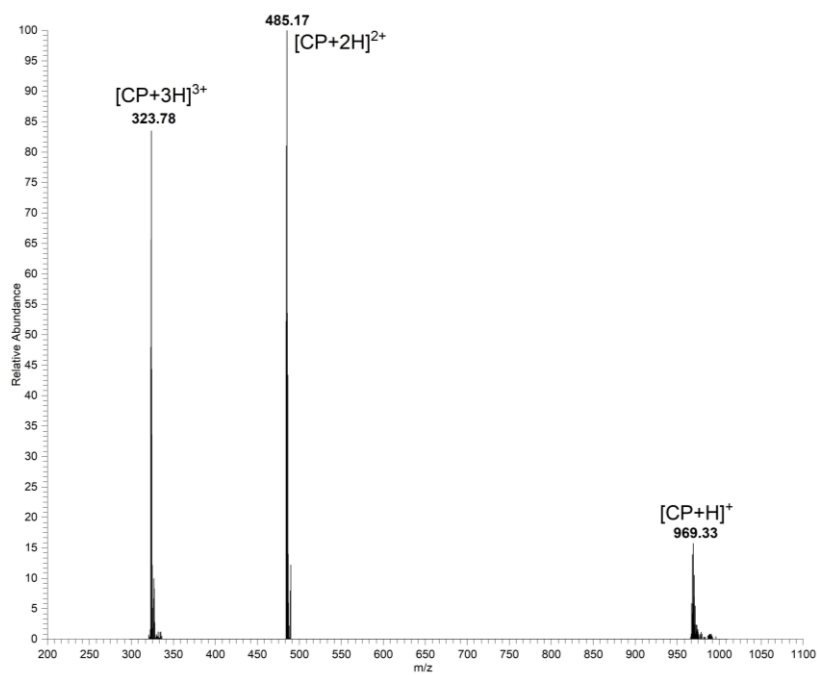


Fig. S3 Mass spectrum of CP.

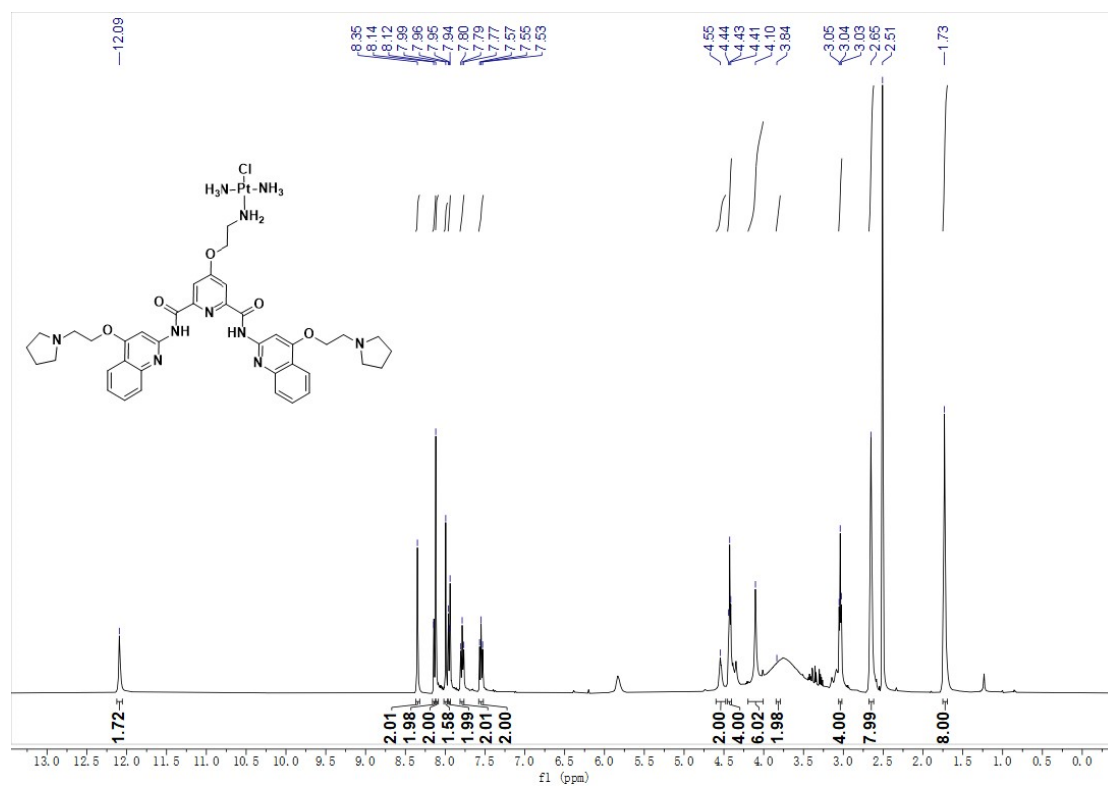


Fig. S4 <sup>1</sup>H NMR spectrum of TP in DMSO-*d*<sub>6</sub> at 25 °C.

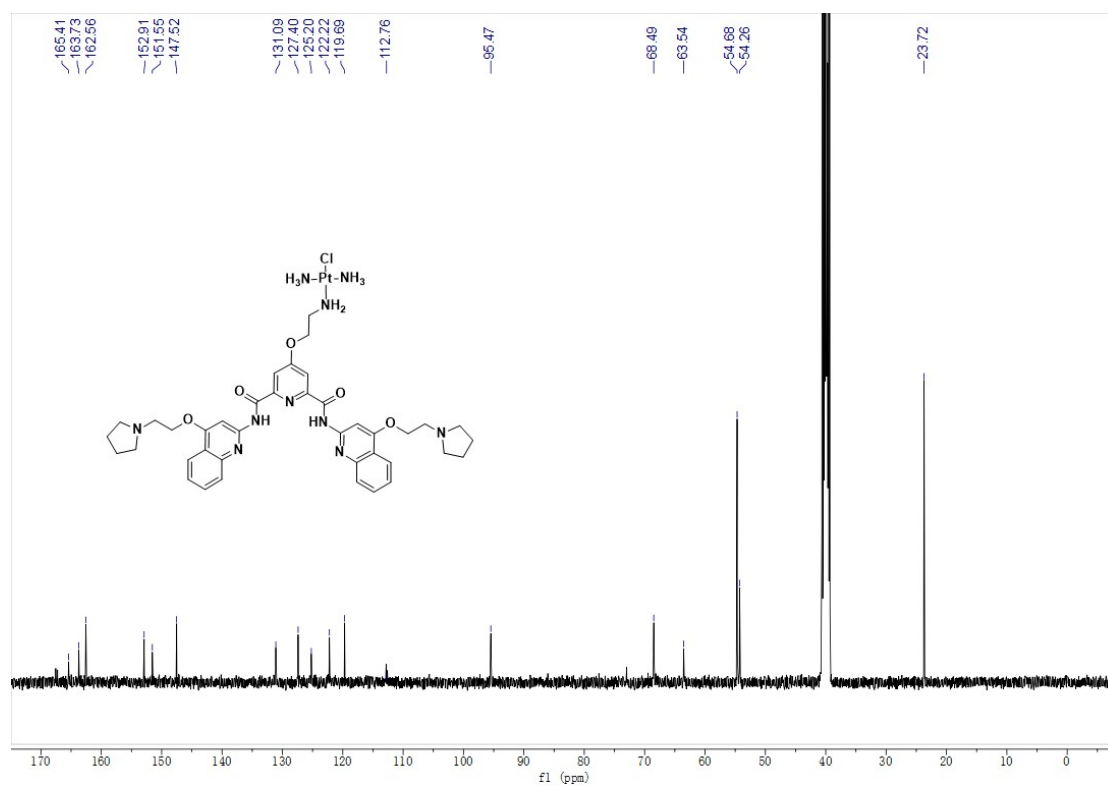


Fig. S5  $^{13}\text{C}$  NMR spectrum of TP in  $\text{DMSO-}d_6$  at 25 °C.

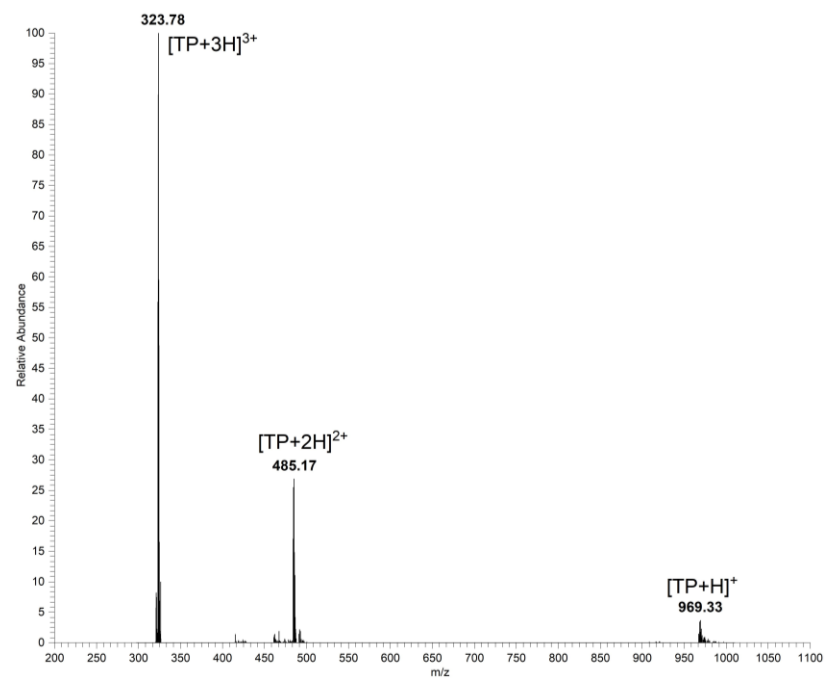
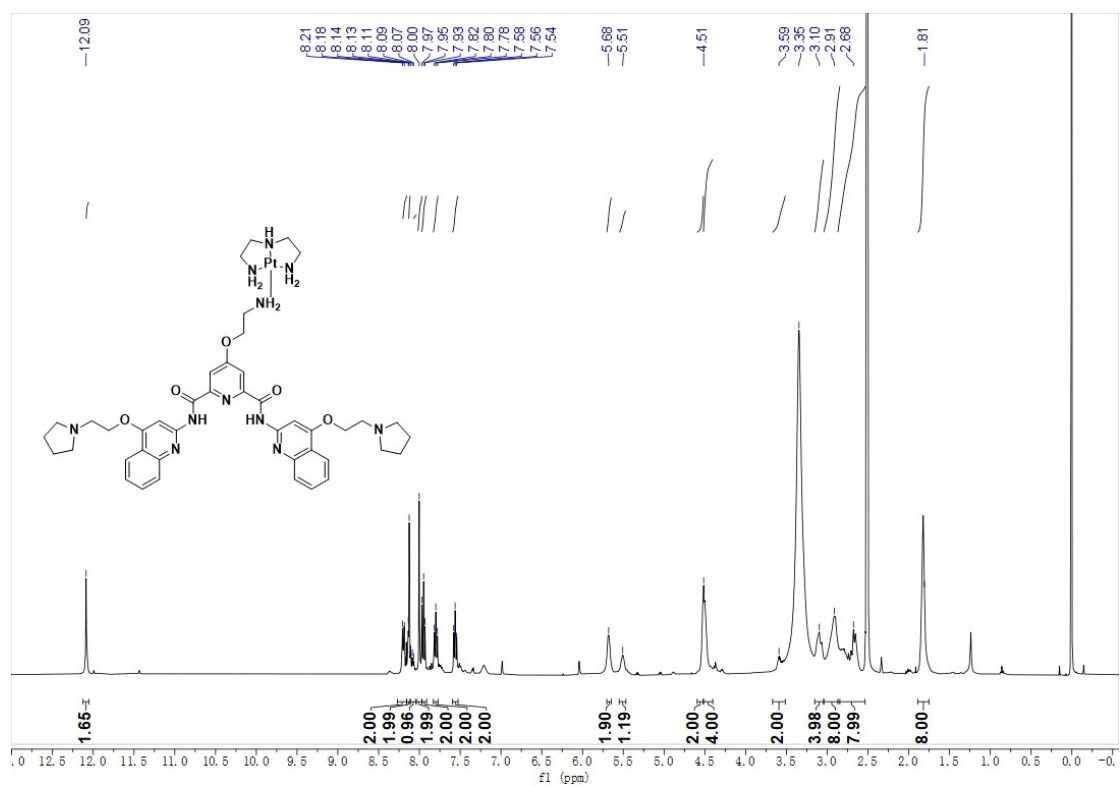
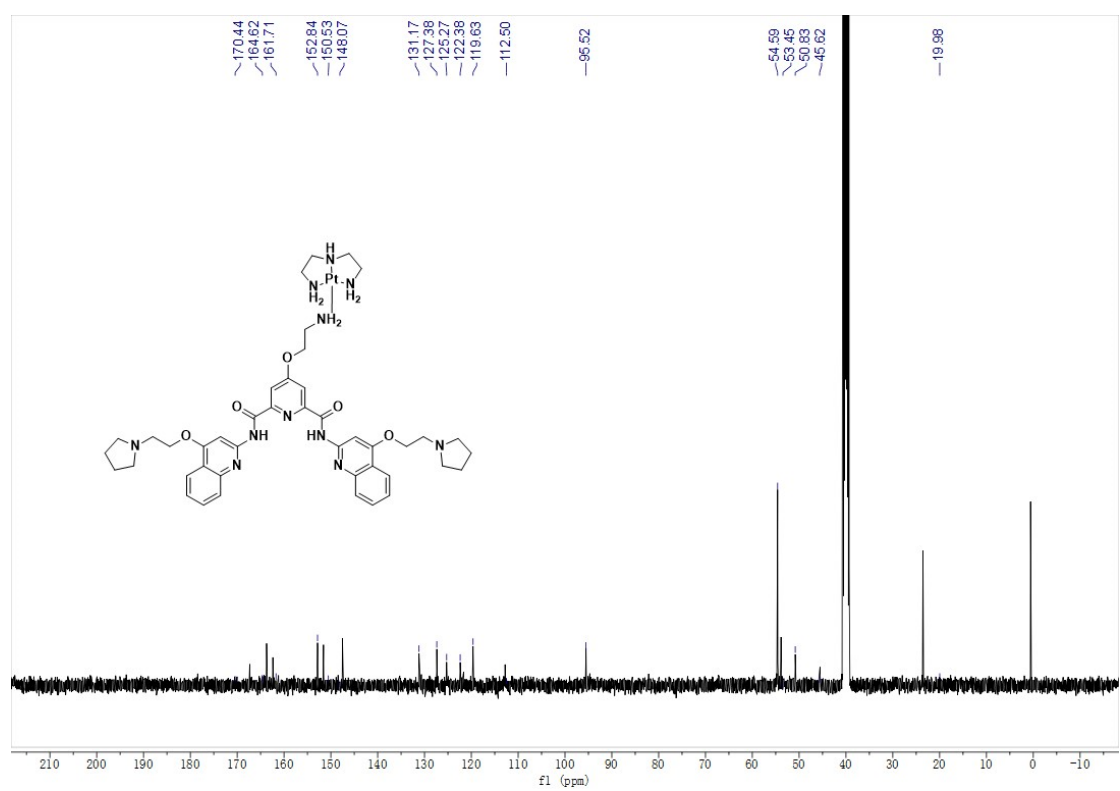


Fig. S6 Mass spectrum of TP.



**Fig. S7** <sup>1</sup>H NMR spectrum of DP in DMSO-*d*<sub>6</sub> at 25 °C.



**Fig. S8** <sup>13</sup>C NMR spectrum of DP in DMSO-*d*<sub>6</sub> at 25 °C.

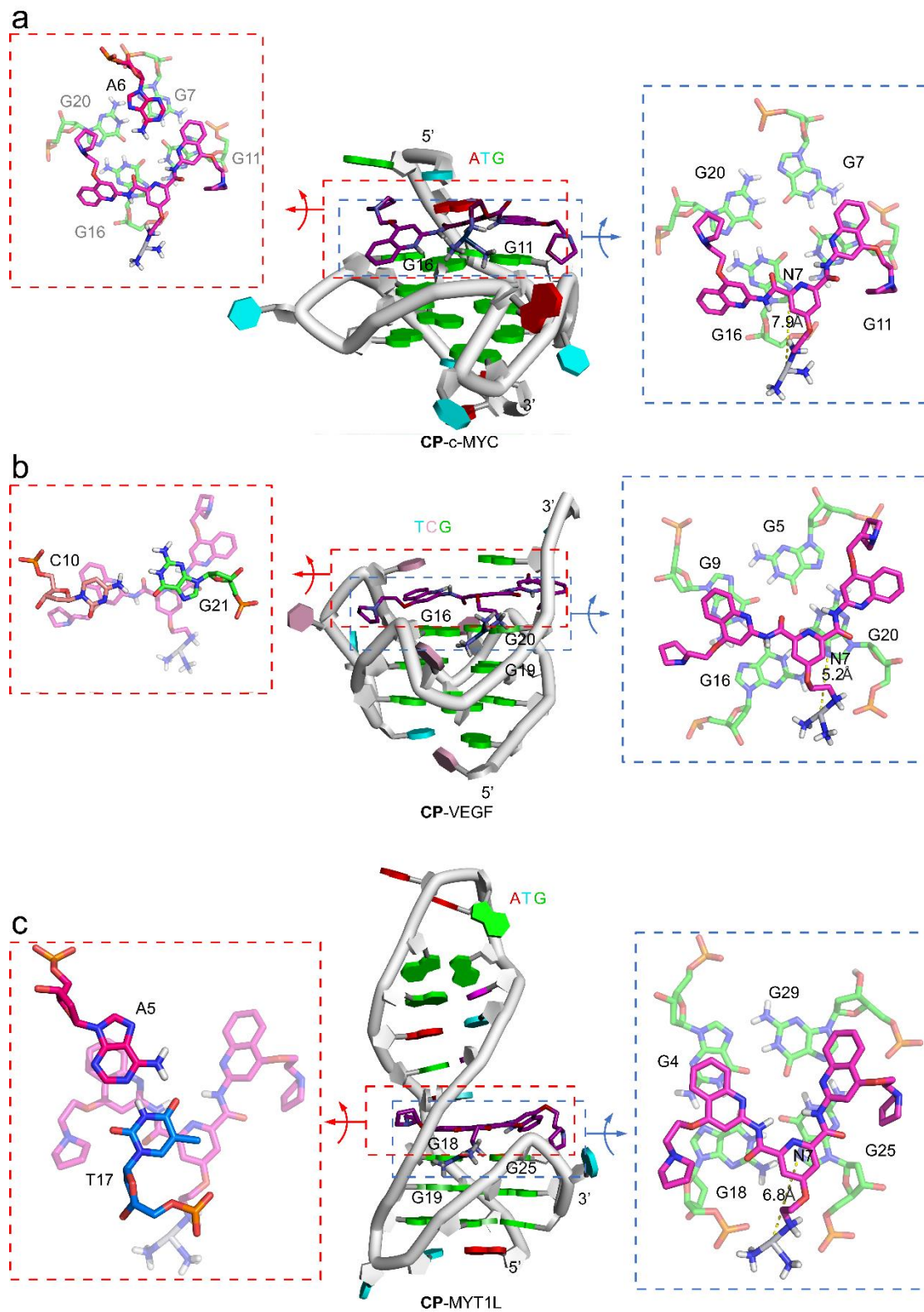


**Fig. S9** Representative structures of the 1:1 CP with c-MYC, VEGF and MYT1L G4 complexes.

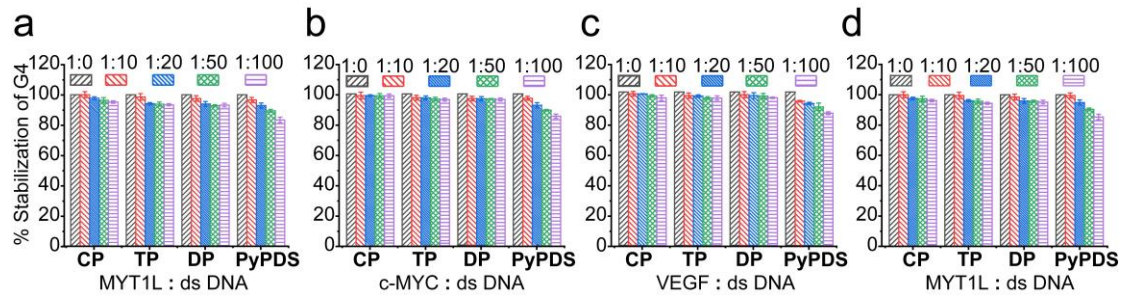


**Fig. S10** (a) Thermal stabilization of MYT1L G4 with **CP**, **TP**, **DP** and **PyPDS** while competing with increasing ratios of ds-12CT for binding to ligands. After mixing the compound and DNA, the samples were tested immediately. (b-d) Thermal stabilization of c-MYC, VEGF and MYT1L G4s after 48 h interacting with **CP**, **TP**, **DP** and **PyPDS** while competing with increasing ratios of dsDNA for binding to ligands. “G4”, meaning “c-MYC, VEGF and MYT1L”, and “dsDNA”, meaning “ds-12CT DNA”.

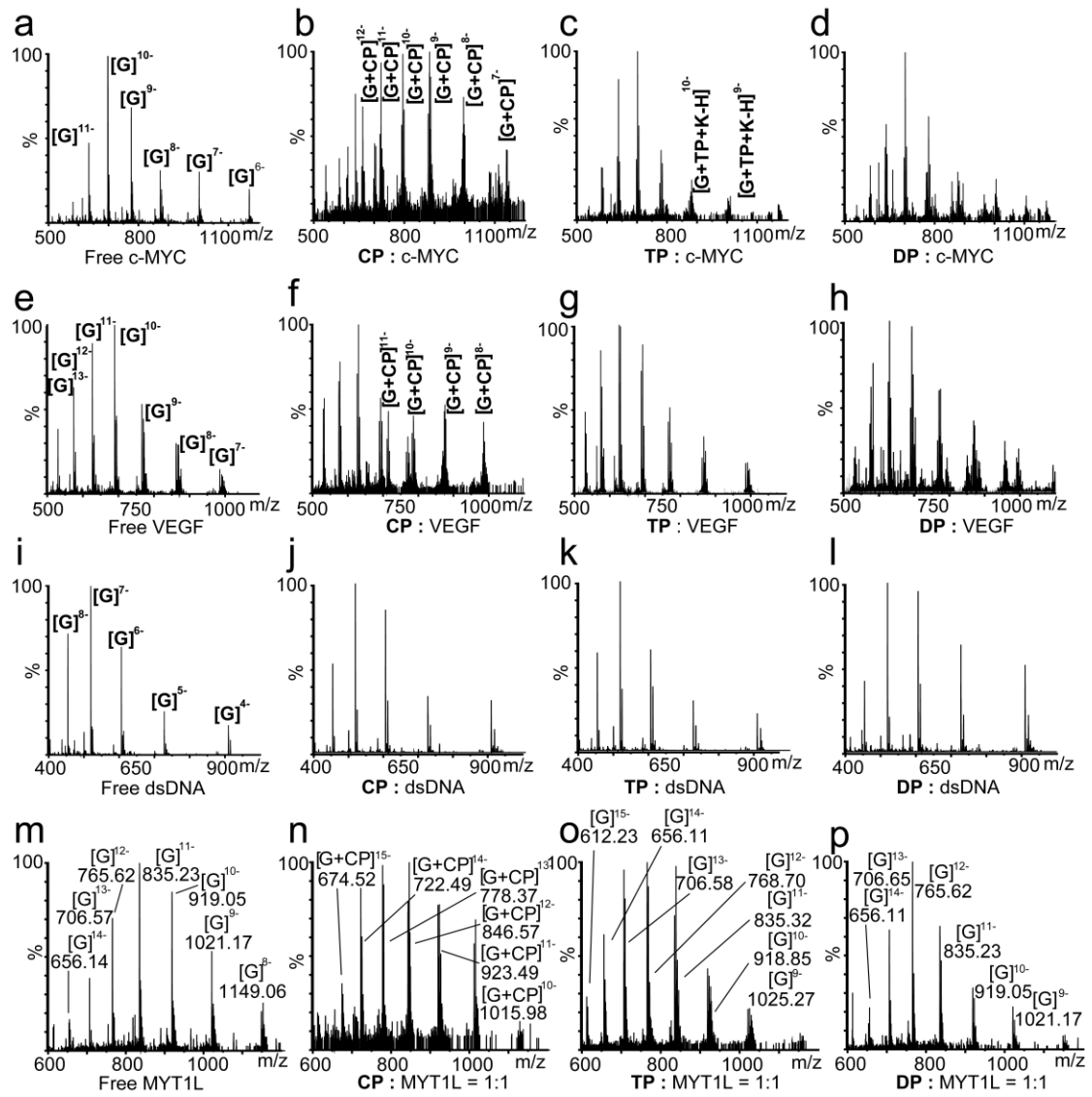


**Fig. S11** (a-p) ESI-MS of c-MYC, VEGF, MYT1L G4s and dsDNA interacting with CP, TP and DP. The peaks are labeled with “G”, meaning “c-MYC, VEGF and MYT1L”, and “dsDNA”, meaning “ds-12CT DNA”. CP, TP and DP: G = 1 : 1.

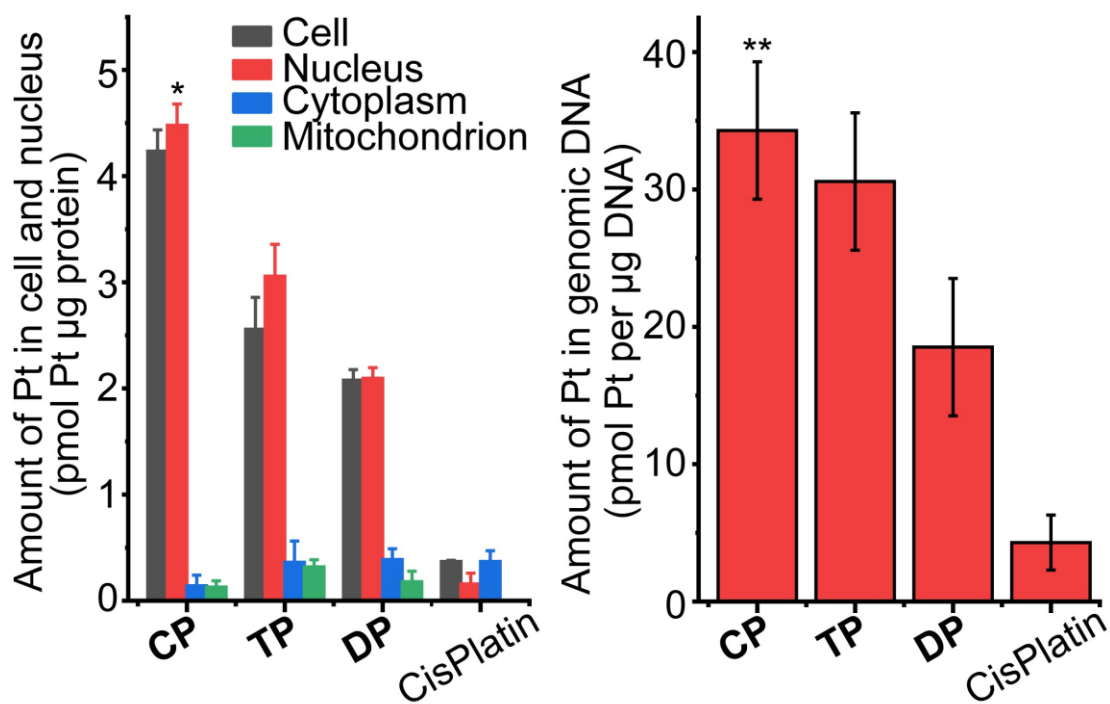


**Fig. S12** The amount of Pt in cell, nucleus and the amount of Pt in the genomic DNA of MDA-MB-231 cells after treated with different concentrations of **CP**, **TP** and **DP** for 24 h. Compound incubation concentration **CP**: 3 µM, **TP**: 3 µM, **DP**: 6 µM and **PyPDS**: 6 µM. Errors are s.d. (n≥3). \*p<0.05, \*\*p<0.01.

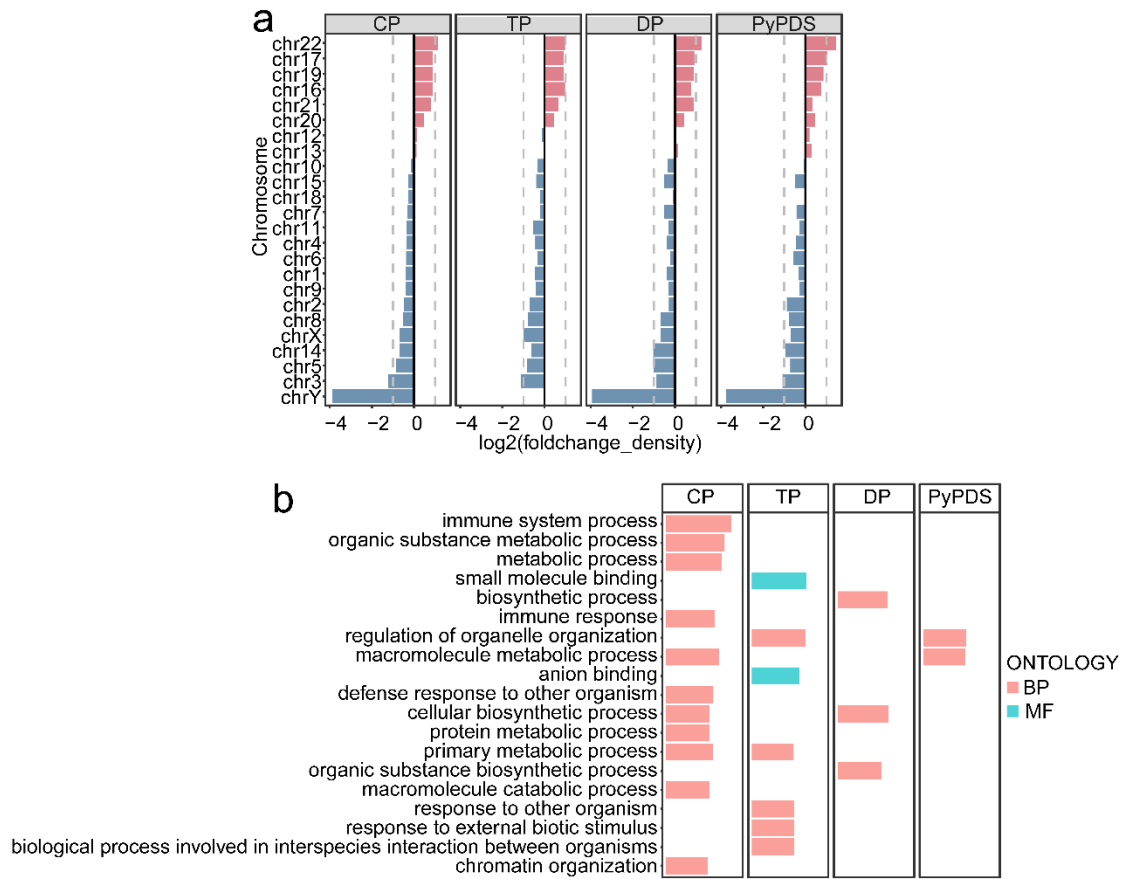


**Fig. S13** Distribution on chromosomes and GO enrichment of target gene.

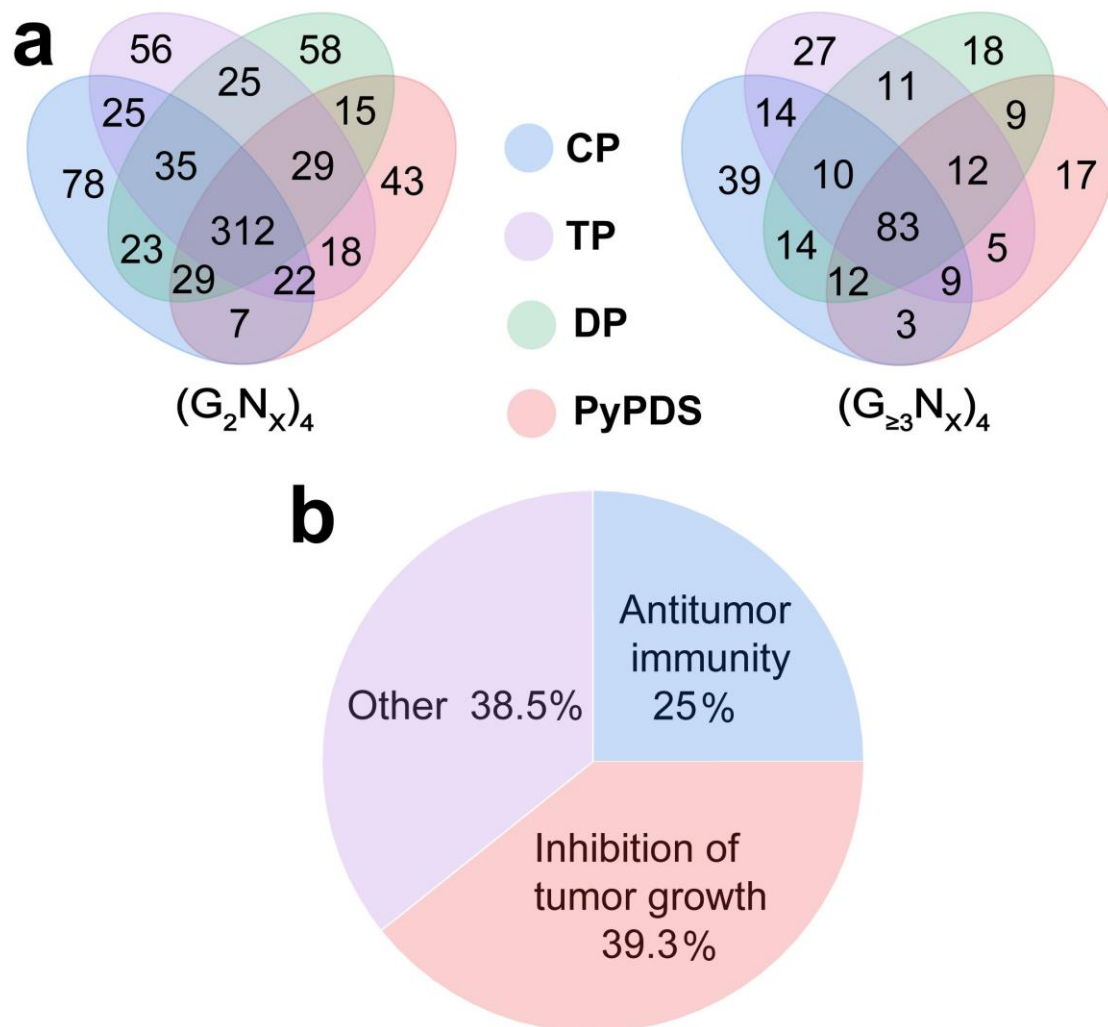


**Fig. S14** (a) Venn diagram of the effects of compounds on genes. (b) Pie chart of the proportion of G4 deletions in whole-genome sequencing in the **CP** group.

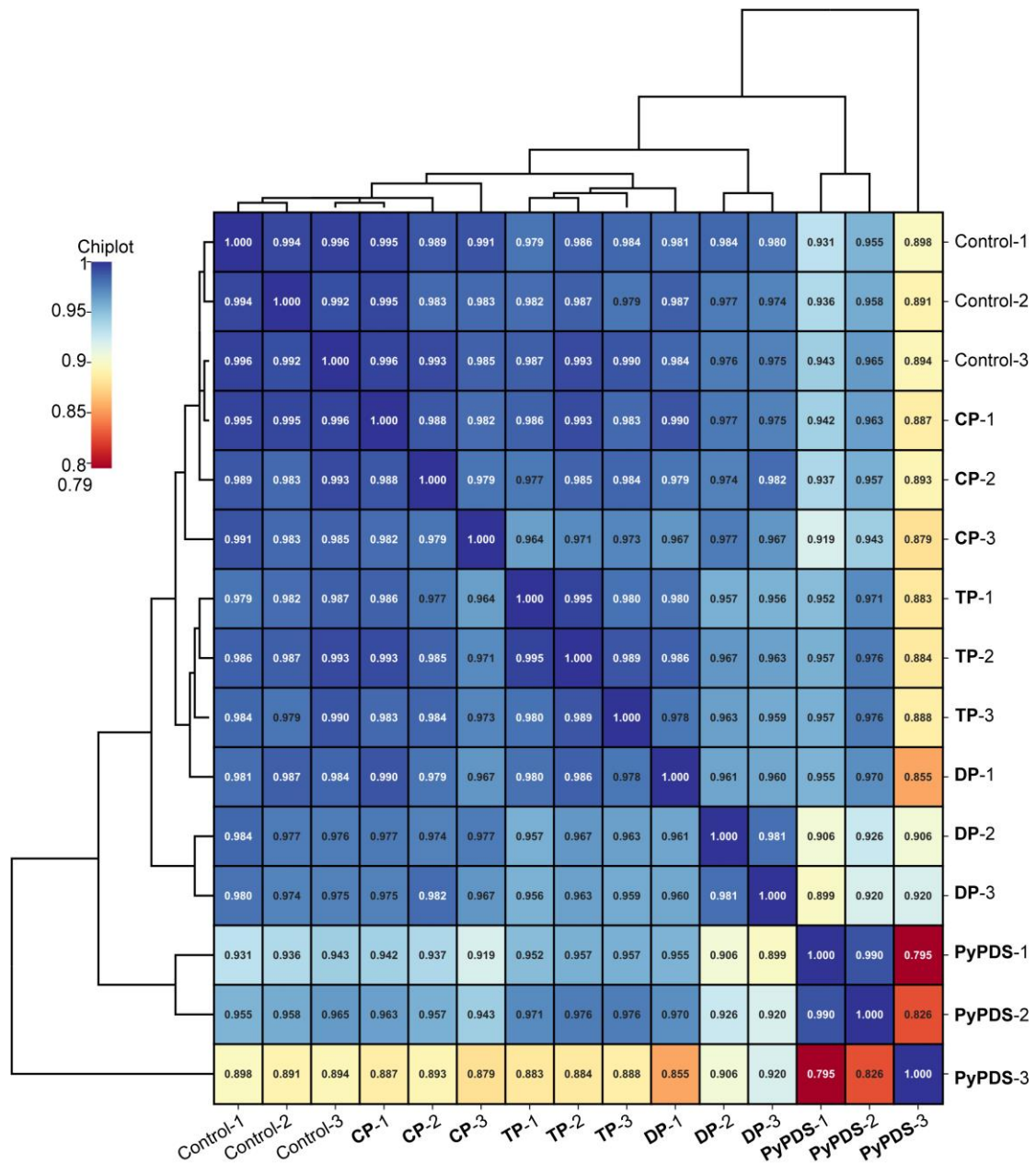


**Fig. S15** Heatmap diagram of Pearson correlation coefficients between the RNA-seq samples. Cell samples were treating with **CP**, **TP**, **DP**, and **PyPDS**, respectively, and the reproducibility of the data was confirmed by correlation coefficients (above 0.80) between parallel samples.

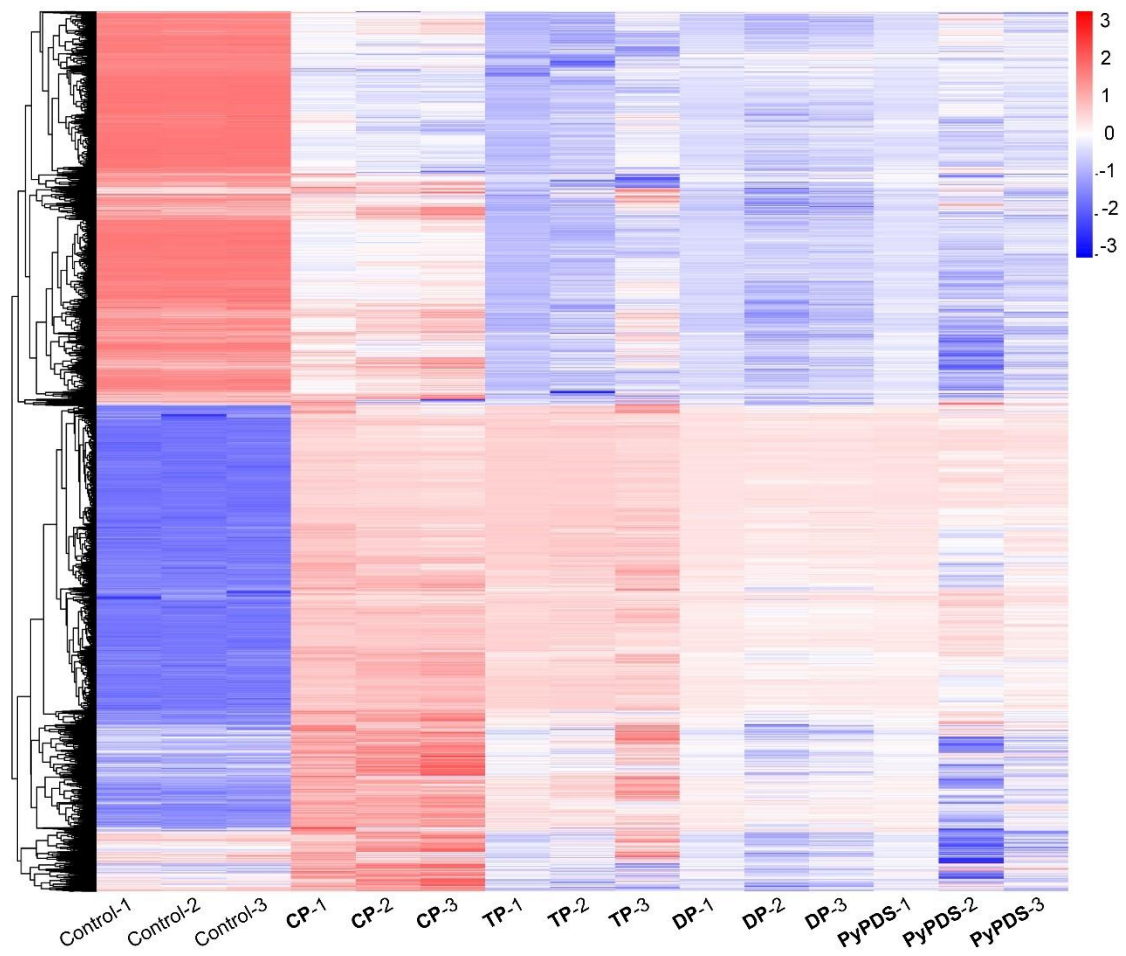


**Fig. S16** Cluster analysis and Heatmap displayed the overview of the differentially expressed genes (DEGs) induced by **CP**, **TP**, **DP** and **PyPDS** for 24 h. RNA-seq clustering heatmaps showed that the expression patterns of transcription treatment groups of **CP** and **TP** were similar, but different from those of **DP** and **PyPDS** groups, indicating that the cellular response mechanisms of **CP** and **TP** group transcription were comparable.

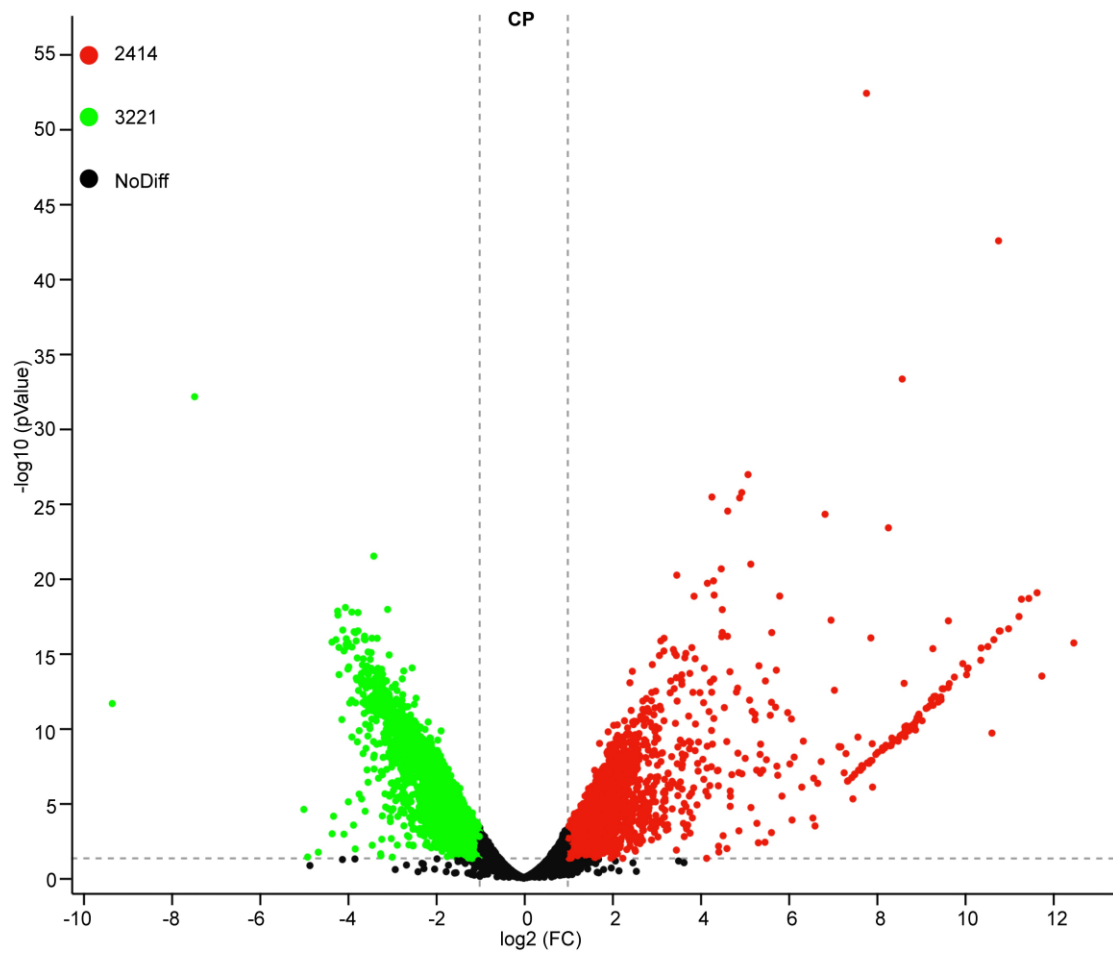


**Fig. S17** Volcano plots showing the DEGs in MDA-MB-231 cells treated with CP for 24 h.

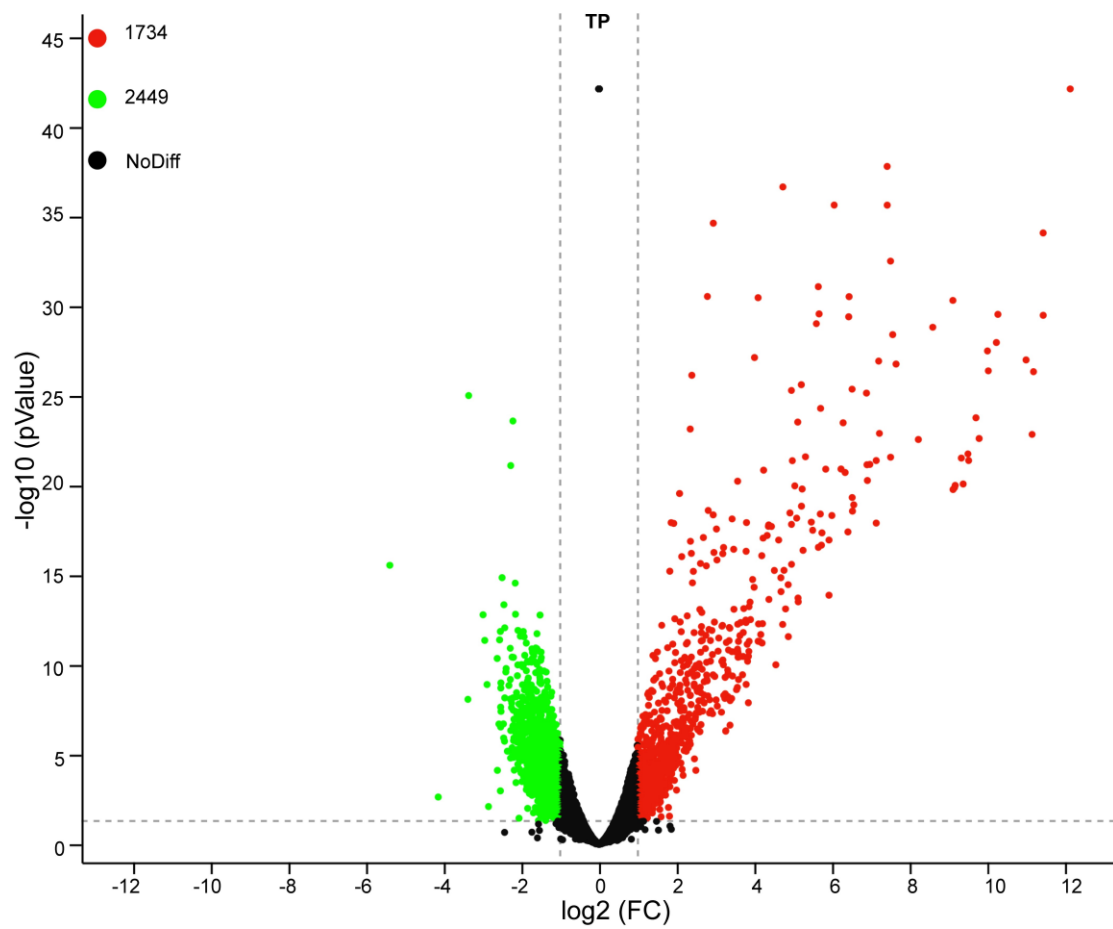


**Fig. S18** Volcano plots showing the DEGs in MDA-MB-231 cells treated with TP for 24 h.

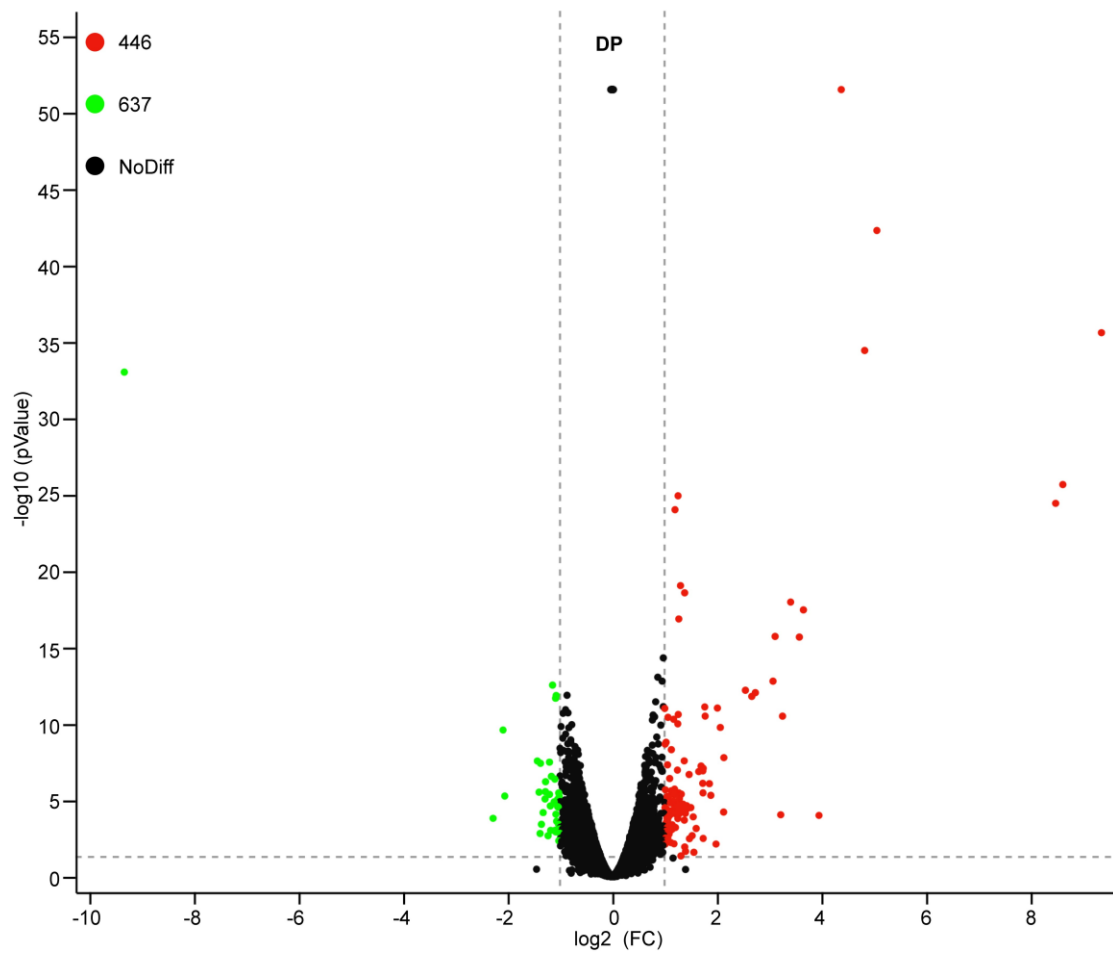


**Fig. S19** Volcano plots showing the DEGs in MDA-MB-231 cells treated with DP for 24 h.

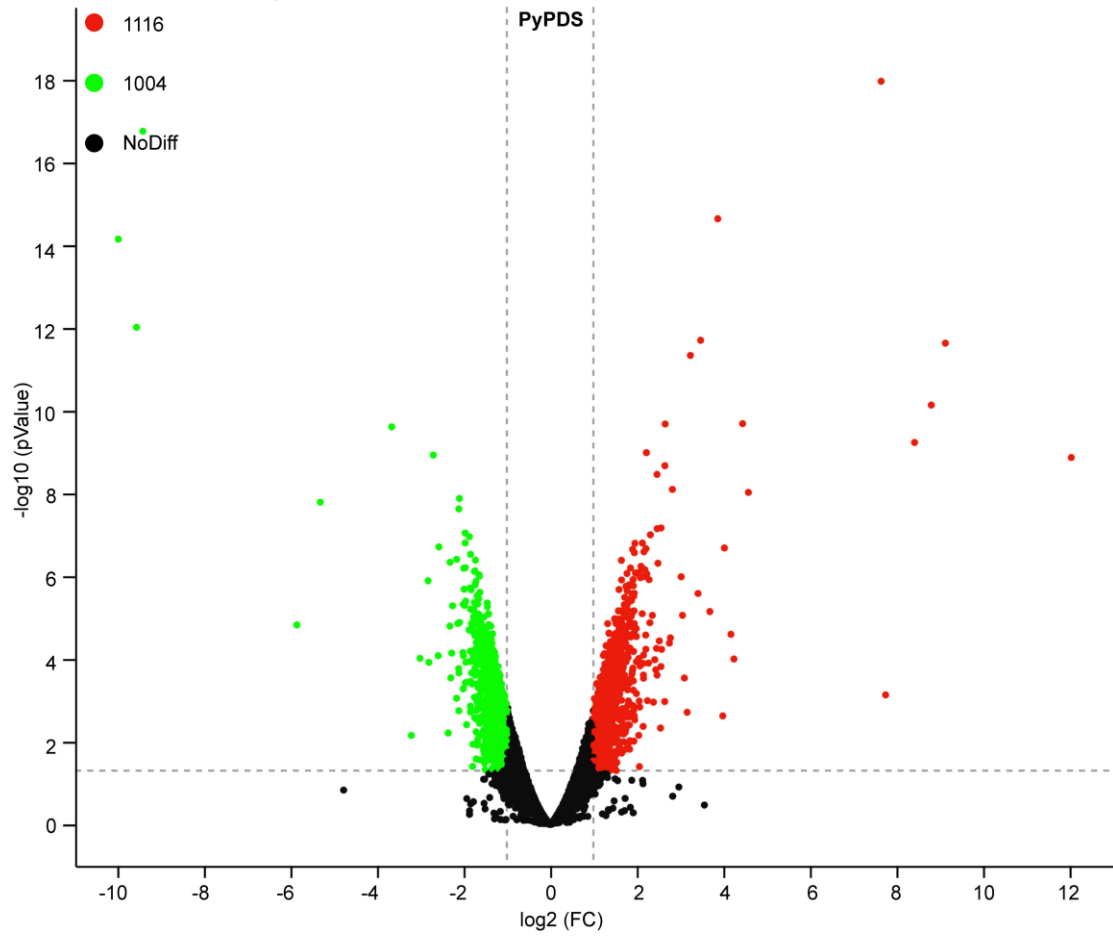


**Fig. S20** Volcano plots showing the DEGs in MDA-MB-231 cells treated with **PyPDS** for 24 h.

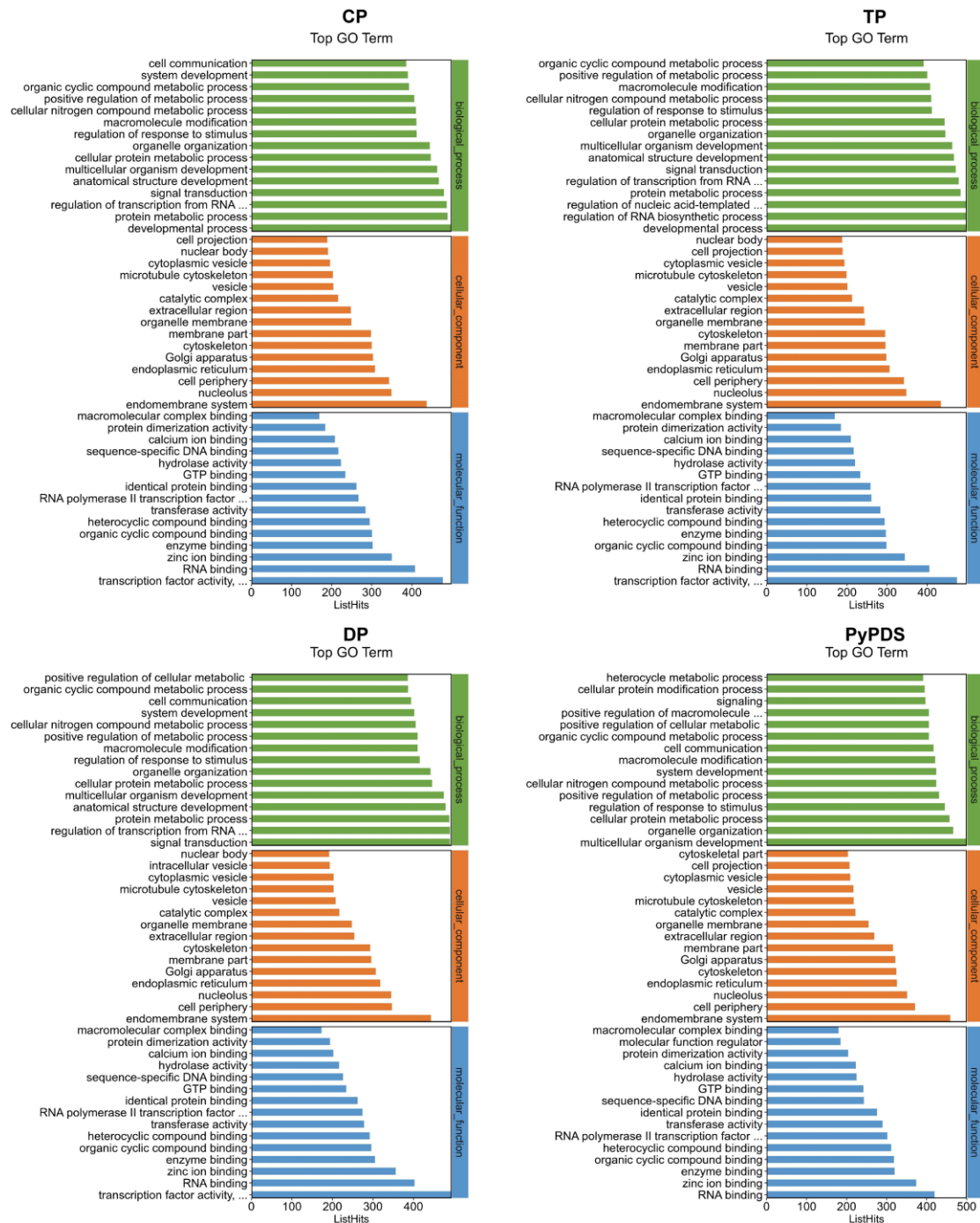
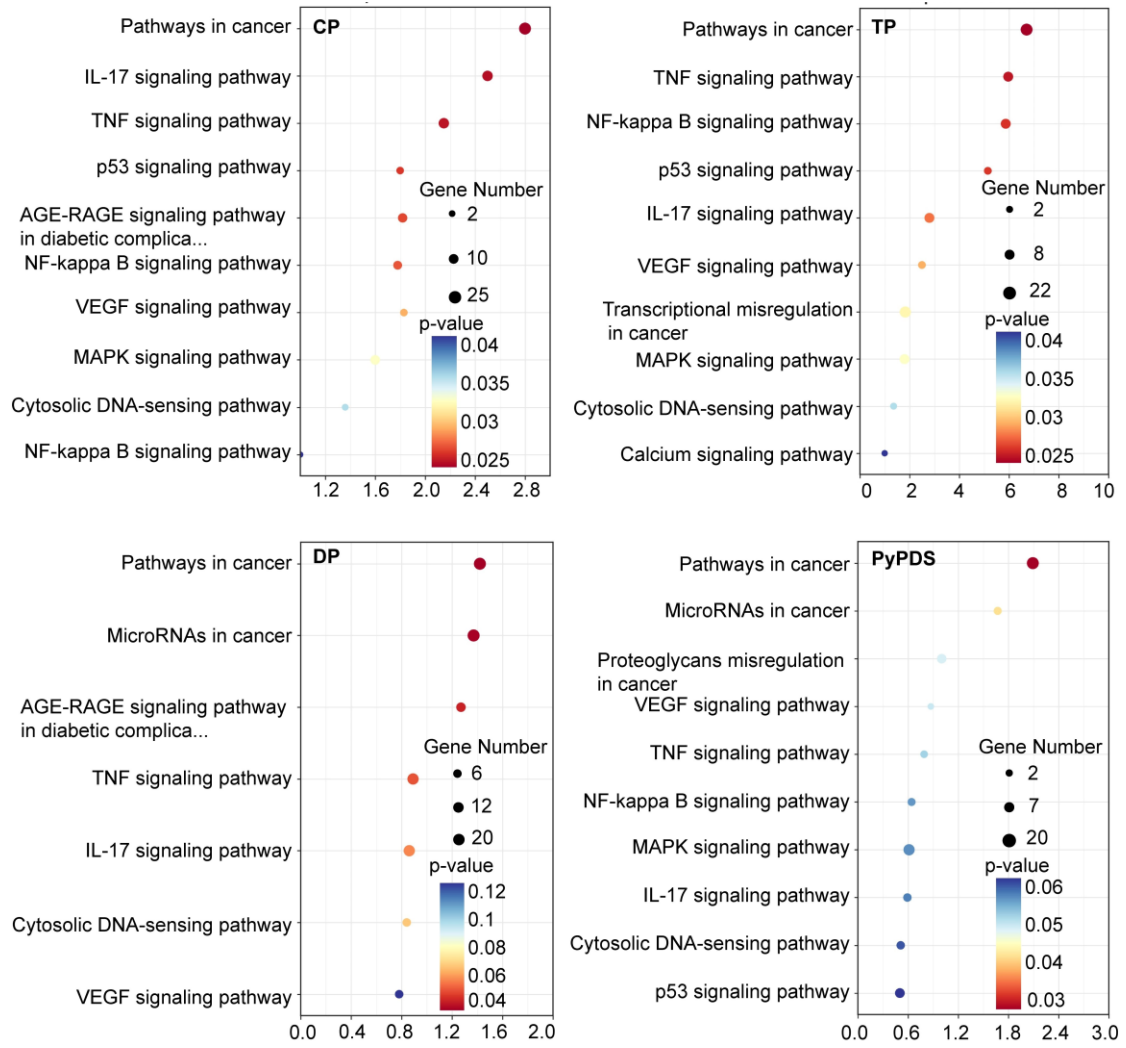
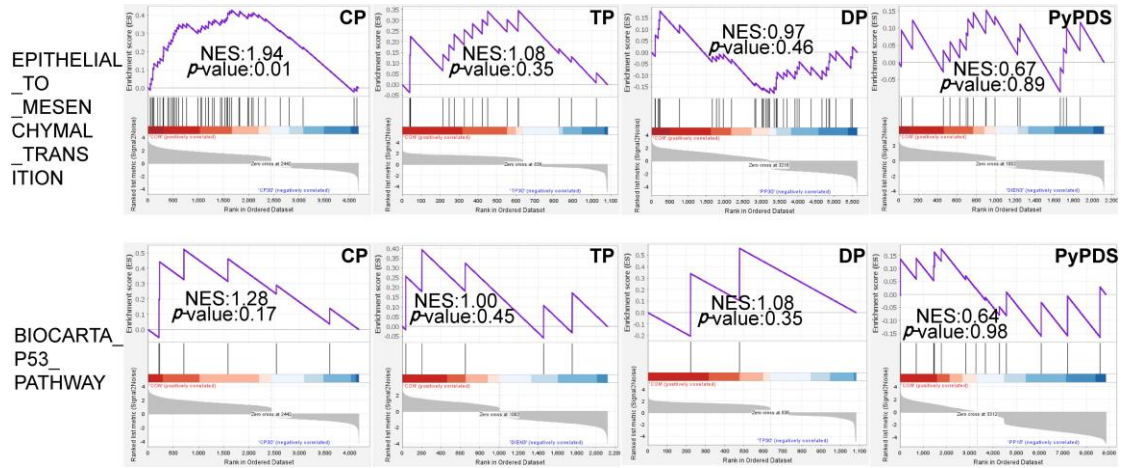


Fig. S21 GO enrichment analysis of DEGs.



**Fig. S22** KEGG enrichment analysis of differentially expressed genes after **CP**, **TP**, **DP** and **PyPDS** treated for 24 h. KEGG enrichment analysis of RNA-seq revealed that **CP**, **TP**, **DP**, and **PyPDS** mainly affected pathways in cancer, cytosolic DNA-sensing, and immunity.



**Fig. S23** GSEA reveals positive enrichment of genes altered in cells subjected after CP, TP, DP and PyPDS treated.

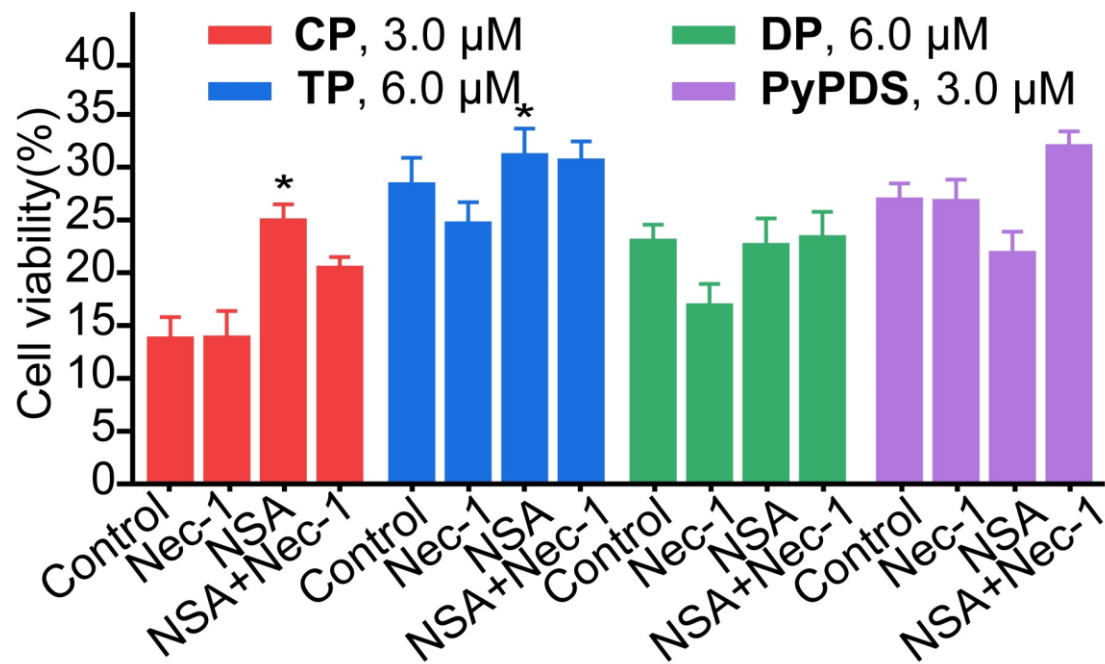


**Fig. S24** The impact of different inhibitors on cell death induced by compounds. Cells were pretreated with the inhibitors (Nec-1: 100 μM; NSA: 10 μM) for 1 h and then subjected to compound treatment. Errors are s.d. (n ≥ 3). \*p < 0.05.

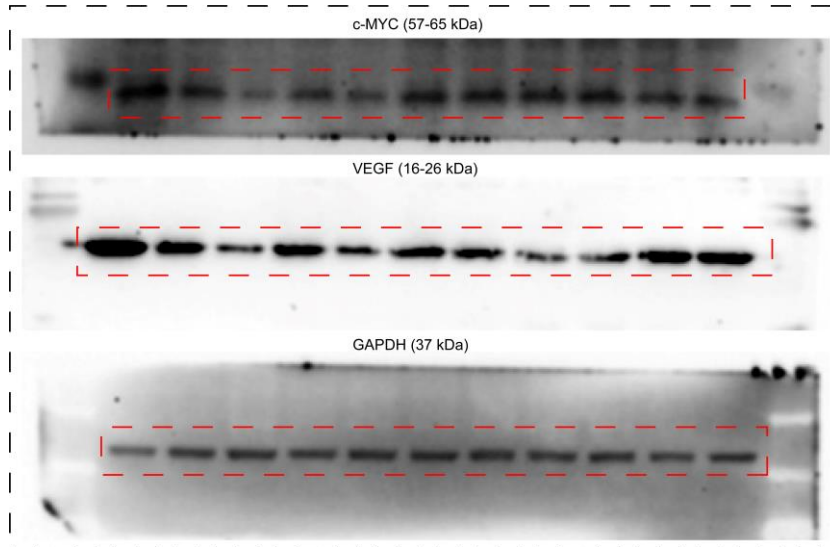


**Fig. S25** Un-cropped western blotting images of Figure 2f.

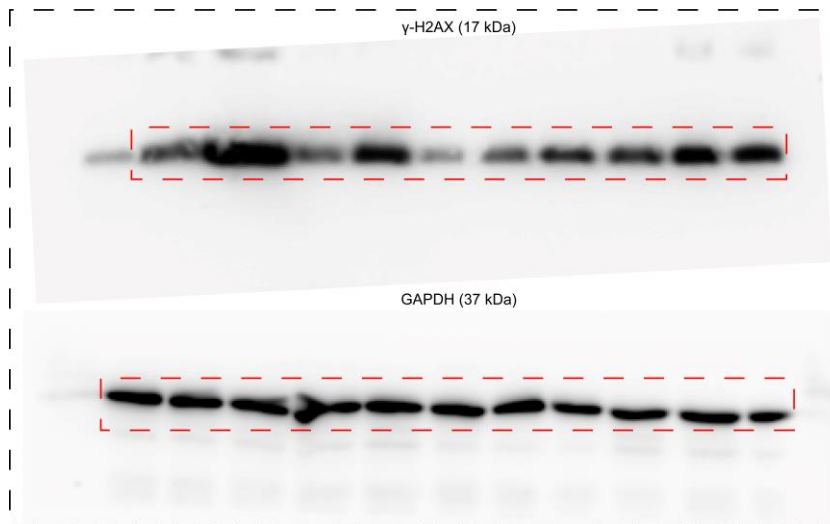


**Fig. S26** Un-cropped western blotting images of Figure 3g.

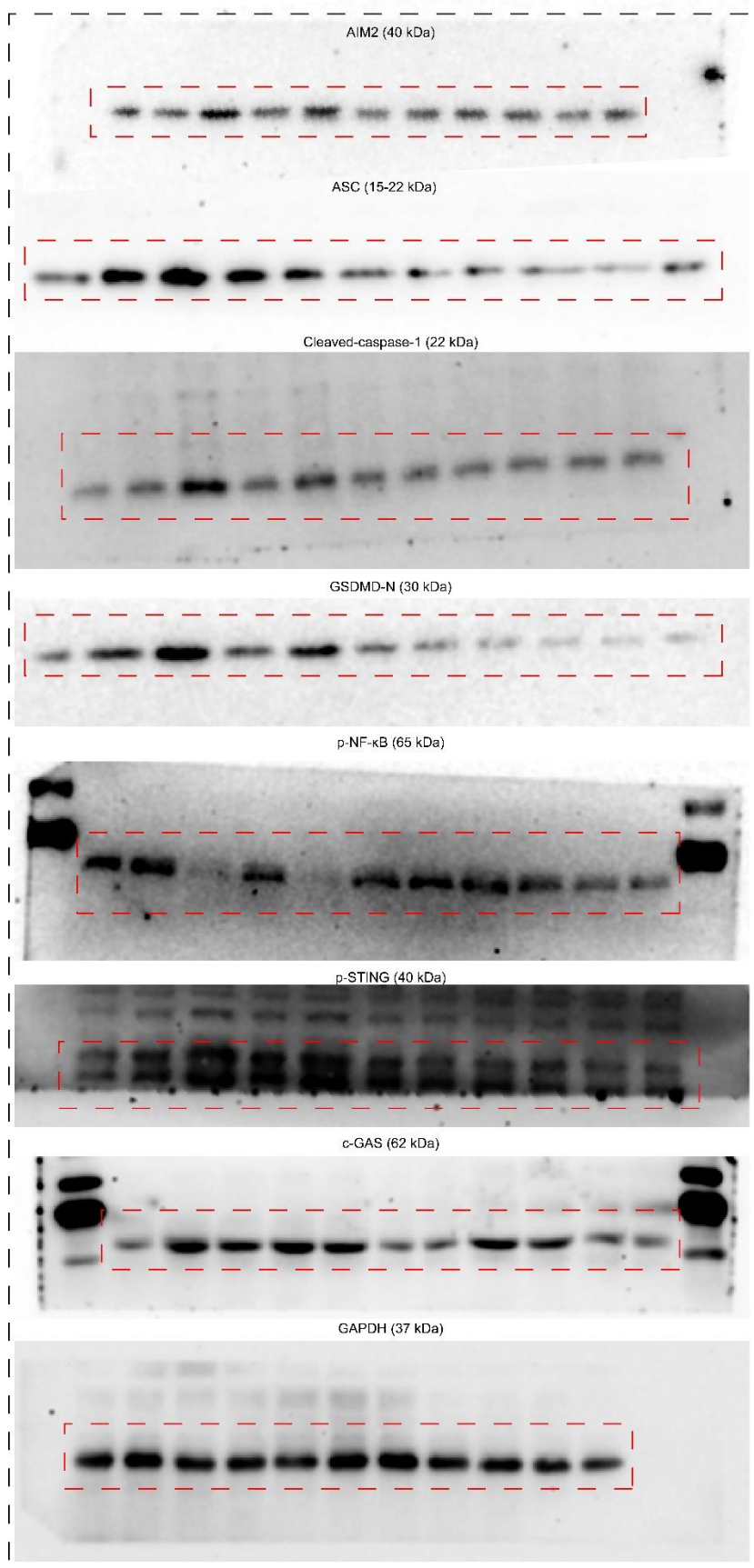


**Fig. S27** Un-cropped western blotting images of Figure 4g.

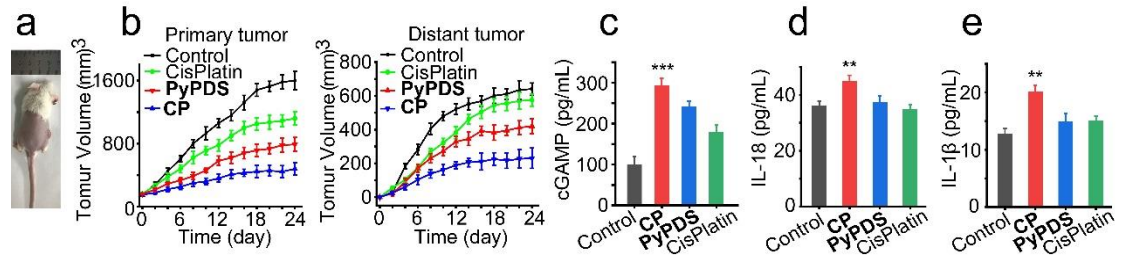


**Fig. S28** (a) Representative photographs of mice in the CP group at 24 days before sacrifice. (b) Volume changes of primary and distant tumors (n=4). Errors are s.d. (n≥3). (c-e) the secretion of cytokines (cGAMP, IL-18 and IL-1β) in serum on Day 16. \*\*p<0.01, \*\*\*p<0.001.

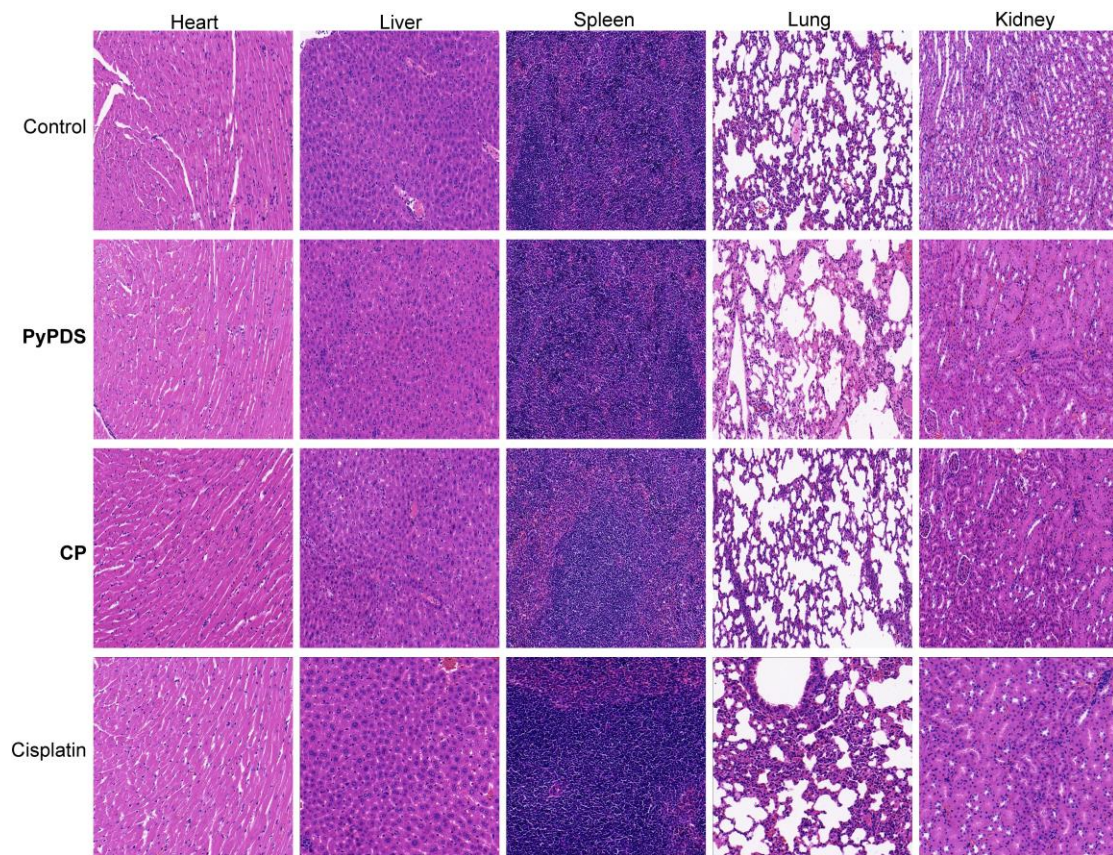


**Fig. S29** Hematoxylin and eosin (H&E) staining of the main organs from mice with different treatment.

**Table S1** The representative docked free energies of the docking models between **CP** and c-MYC G4 DNA.

Number of AutoDock clusters a	Docked free energy range of docked structures (kcal/mol)	Cluster rank b	Docked free energy (kcal/mol)
39(100)	-10.67 to -4.64	1	-10.67
		2	-10.27
		3	-10.22
		4	-10.08
		5	-10.04
		6	-10.01
		7	-9.79
		8	-9.74
		9	-9.53
		10	-9.48

a. Number of GA runs are shown in parentheses. B. The cluster rank is the absolute ranking as determined by the docked free energy defined by AutoDock.

**Table S2** The representative docked free energies of the docking models between **CP** and VEGF G4 DNA.

Number of AutoDock clusters a	Docked free energy range of docked structures (kcal/mol)	Cluster rank b	Docked free energy (kcal/mol)
66 (100)	-11.51 to -5.06	1	-11.51
		2	-10.99
		3	-10.82
		4	-10.00
		5	-9.84
		6	-9.77
		7	-9.69
		8	-9.60
		9	-9.01
		10	-8.89

a. Number of GA runs are shown in parentheses. b. The cluster rank is the absolute ranking as determined by the docked free energy defined by AutoDock.

**Table S3** The representative docked free energies of the docking models between CP and MYT1L G4 DNA.

Number of AutoDock clusters a	Docked free energy range of docked structures (kcal/mol)	Cluster rank b	Docked free energy (kcal/mol)
85 (100)	-15.50 to -6.7	1	-15.50
		2	-14.10
		3	-14.00
		4	-13.73
		5	-13.67
		6	-13.08
		7	-12.92
		8	-12.91
		9	-12.80
		10	-12.54

a. Number of GA runs are shown in parentheses. b. The cluster rank is the absolute ranking as determined by the docked free energy defined by AutoDock.

**Table S4.** List of DNA sequences used in this research.

Name	Sequence
c-MYC	5'-TGAGGGTGGGTAGGGTGGGTAA-3'
VEGF	5'-CGGGGCGGGCCTTGGGCGGGGT-3'
MYT1L	5'-AGGGAGAGGAGAGCTCTGGGTTGGGTGGG-3'
ds-12CT	5'-CTTTTGCAAAG-3'
ds-26	5'-CAATCGGATCGAATTCGATCCGATTG-3'

**Table S5.** The nearest gene of ChromHMM annotation

Roadmap	Standardized Epigenome name	AGE (Years)	SEX	ETHNICITY
E027	Breast Myoepithelial Primary Cells	36Y,33Y	Female	African-American, African-American
E028	Breast variant Human Mammary Epithelial Cells (vHMEC)	18Y	Female	Caucasian
E119	Human Mammary Epithelial Primary Cells (HMEC)	Unknown	Unknown	Unknown

**Table S6.** The Quadruplex forming G-Rich Sequences (QGRS) in the significant enrichment genes associated with G4 deletions in the **CP** group.

	Gene Name	CDH4	SNTG2	GRTP1	C7orf50	ATP9B	CIMAP1D	COL18A1	MIR3667HG	EARP	NGEF	
<b>CP</b>	QGRS in full gene sequence	6129	2313	365	1511	1468	113	1345	2133	1460	976	
	QGRS in promoter sequence	17	17	23	23	24	21	31	24	16	19	
		Gene Name	IGSF21	LARGE1	SLC16A3	COL6A1	MUC4	C4orf19	PADI4	c-MYC	DHRXS	VEGF
	QGRS in full gene sequence	2311	4473	518	338	592	882	493	74	1916	207	
QGRS in promoter sequence	20	27	32	15	29	8	16	17	21	24		

**Table S7.** The **CP** group had the highest proportion of G4 deletions in whole-genome sequencing.

Inhibition of tumor growth	SOX6	LAMA5	APP	URB1	DIP2C	c-MYC
	GNAQ	BRSK2	CDH4	MYT1	VEGF	
Antitumor immunity	SYNE2	TNFRSF1A	APLP2	HNF1A	MYO10	TRAPPC9
	LGR4					
Other	PPP2R2C	CACNG7	FBRSL1	PPHLN1	SAXO1	COL26A1
	ANKRD11	ADARB2	NKAIN3	AC000093.1		

**Table S8.** The Quadruplex forming G-Rich Sequences (QGRS) in the genes of which the expression was significantly regulated by **CP**, **TP**, **DP** and **PyPDS** in the RNA-seq studies.

<b>CP</b>	Gene Name	SOX6	AACS	TACC2	CREB3L1	CDH4	ABCA3	CD44	FEZF1	FAM219A	FARP1
	QGRS in full gene sequence	2552	687	2041	427	6129	632	495	66	445	1880
	QGRS in promoter sequence	11	19	15	23	17	26	21	12	30	16
	Gene Name	PIGX	PINK1	PYROXD2	c-MYC	FAM187A	ITGA5	APBB2	CNTNAP1	APOL2	VEGF
QGRS in full gene sequence	620	173	297	74	30	244	2208	199	137	207	
QGRS in promoter sequence	15	13	15	17	14	32	24	18	22	24	
<b>TP</b>	Gene Name	VDR	KANK1	ZHX3	NR3C2	EDN1	CREB3L2	TESMIN	PHACTR4	ZNF329	RTN4
	QGRS in full gene sequence	797	1399	736	1394	42	757	260	720	203	553
	QGRS in promoter sequence	26	13	15	26	10	21	20	15	25	15
	Gene Name	GNL3L	RCBTB1	HERPUD2	RGMB	AMPH	AP1S3	LMO7	CHD8	PAM	SRCAP
QGRS in full gene sequence	504	281	275	170	1005	927	989	401	817	337	
QGRS in promoter sequence	13	13	19	7	18	28	12	17	15	25	
<b>DP</b>	Gene Name	RCN3	NPDC1	PHLDB1	GPAA1	C16orf74	CREB3L1	PPARD	ARHGEF10L	FAM219A	SPEG
	QGRS in full gene sequence	200	117	546	99	577	427	681	1738	445	669
	QGRS in promoter sequence	20	33	13	19	28	23	22	17	30	13
	Gene Name	ZNF213	MAP4	EML2	TBC1D24	ITGA5	CNTNAP1	NXPH4	SLC37A4	PTPN23	TAGLN
QGRS in full gene sequence	144	1380	409	378	244	199	116	86	278	118	
QGRS in promoter sequence	21	22	26	25	32	18	23	24	11	25	

	Gene Name	DPM2	MSRB1	RPS11	PNMA1	RPS17	KRTCAP2	TMEM216	DPY30	SMARCD3	NCBP2-AS2
<b>PyPDS</b>	QGRS in full gene sequence	40	78	50	29	49	41	46	751	431	21
	QGRS in promoter sequence	20	29	14	20	18	17	17	18	12	16
	Gene Name	ATF6B	NDUFS6	TUT1	GCSH	ERAL1	ECHS1	VPS4A	ABCC6	NAPRT	PDCL3
	QGRS in full gene sequence	131	137	148	92	60	106	163	586	69	100
	QGRS in promoter sequence	17	16	13	14	12	14	15	20	30	19

## References

1. L. Y. Liu, T. Z. Ma, Y. L. Zeng, W. T. Liu and Z. W. Mao, Structural Basis of Pyridostatin and Its Derivatives Specifically Binding to G-Quadruplexes, *J. Am. Chem. Soc.*, 2022, **144**, 11878-11887.
2. L. Y. Liu, H. B. Fang, Q. X. Chen, M. H. Y. Chan, M. Ng, K. N. Wang, W. Liu, Z. Q. Tian, J. J. Diao, Z. W. Mao and V. W. W. Yam, Multiple-Color Platinum Complex with Super-Large Stokes Shift for Super-Resolution Imaging of Autolysosome Escape, *Angew. Chem. Int. Ed.*, 2020, **59**, 19229-19236.